2. MERCURY ATMOSPHERIC CHEMISTRY

The GLEMOS modelling activities concerning mercury in the reporting period were focused on study of principal processes governing its cycling in the atmosphere. In particular, a number of sensitivity runs have been performed to evaluate different chemical mechanisms responsible for Hg oxidation in different atmospheric compartments. The simulation results were compared with detailed measurements from various field campaigns.

2.1. Model updates

A number of the model updates have been performed before the main simulation program. The updates include improvements of the model parameterisation with regard to Hg oxidation chemistry with reactive halogens (mostly, atomic Br) and refinement of the model output to take into account vertical distribution of Hg concentration in the near surface air.

Update of halogen chemistry. The GLEMOS chemical scheme was updated to improve the model description of Hg reactions with atomic Br, which is expected to be a dominant oxidant of Hg in the global atmosphere. In particular, the gas-phase mechanism of Hg oxidation by Br was replaced by more extensive chemical scheme based on the mechanism suggested by *Holmes et al*. [2010]. Gas-phase reactions of Hg with atomic Br included into the updated chemical scheme are presented in Table 2.1 along with the reaction constants and appropriate references.

Table 2.1. Gas*-phase chemical reactions of Hg with atomic Br implemented in GLEMOS*

Reaction	Rate constant, s^{-1}	Reference
$Hg^0 + Br + M \rightarrow HgBr + M$	$1.5 \cdot 10^{-32}$ $(T/298)^{-1.86}$ [Br][M][(a)]	*Donohoue et al*. [2006]; *Goodsite et al*. [2012]
$HgBr \xrightarrow{M} Hg^0 + Br$	$4 \cdot 10^9 \exp(-7292/T)$	*Goodsite et al*. [2012]
$HgBr + Br \rightarrow Hg^0 + Br_2$	$3.9 \cdot 10^{-11}$ [Br]	*Balabanov et al*. [2005]
$HgBr + Br \xrightarrow{M} HgBr_2$	$2.5 \cdot 10^{-10}$ $(T/298)^{-0.57}$ [Br]	*Goodsite et al*. [2004]
$HgBr + OH \xrightarrow{M} HgBrOH$	$2.5 \cdot 10^{-10}$ $(T/298)^{-0.57}$ [OH]	*Goodsite et al*. [2004]

[(a)] All concentrations in brackets are in molecule cm^{-3}; [M] is the number density of air.

In addition, a new set of input data for reactive halogens (Br and BrO) concentration in the atmosphere was incorporated into the model to support simulation of the Hg/halogen chemistry. In particular, 3D fields of Br and BrO with 6-hour temporal resolution archived from the p-TOMCAT model [*Yang et al.,* 2005] were interpolated into the model native grid and utilized for simulations. Spatial distribution of annual mean concentration of Br and BrO on a global scale is shown in Fig. 2.1. As seen high concentrations of both Br and BrO are characteristics of the polar and sub-polar regions. In temperate latitudes the surface Br/BrO concentrations are relatively low. It should be mentioned, however, that in these estimates Br/BrO were simulated with biogenic bromocarbon and methyl bromide as the only source gases, whereas bromine production from sea-salt bromide did not taken into account [*Yang et al*., 2005]. Therefore, these data are not applicable for simulation of the Hg/bromine chemistry in the marine boundary layer.

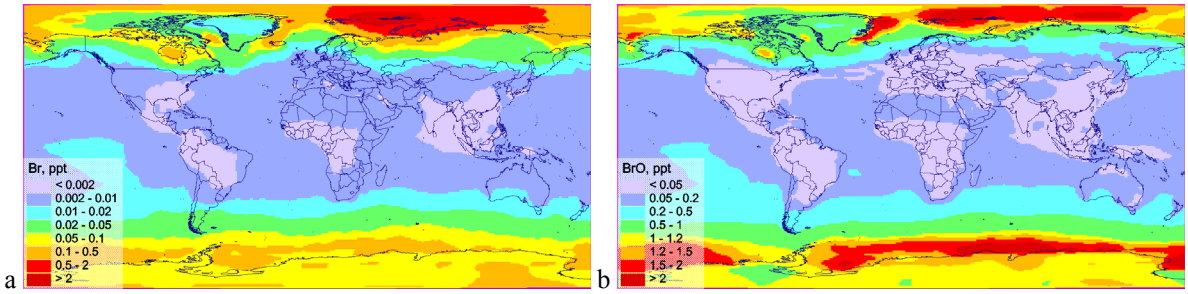

Fig. 2.1. *Spatial distribution of Br (a) and BrO (b) annual mean concentration in the surface air simulated by the p-TOMCAT model.*

Seasonal variation of Br and BrO concentrations in the surface air at different latitudes is illustrated in Fig. 2.2. Both substances have a pronounced maximum (over 1 ppt) in spring and in autumn over the northern and southern poles, respectively. Over the tropics and moderate latitudes yearly variation of Br and BrO is insignificant. In general, concentrations of BrO are higher than Br concentrations in the surface air by an order of magnitude.

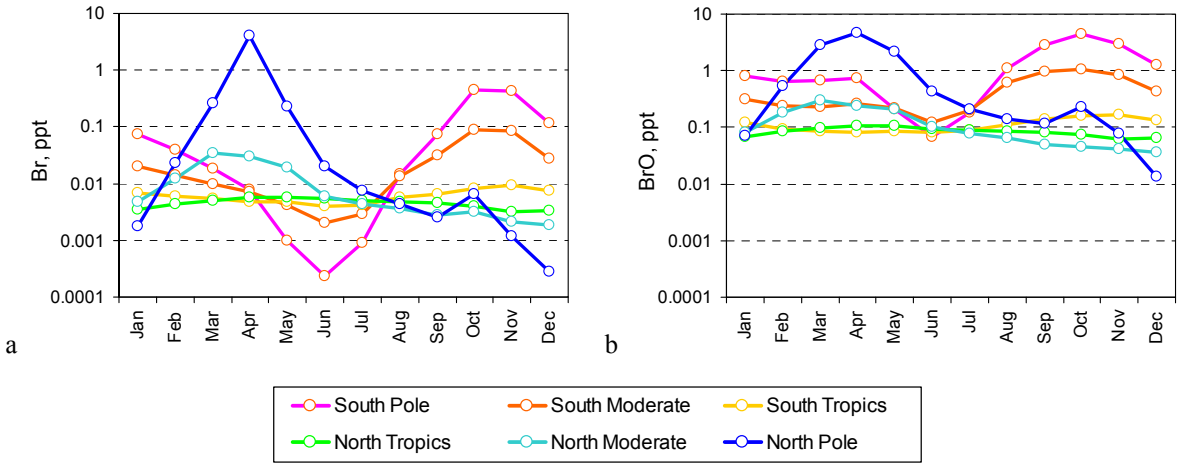

Fig. 2.2. *Seasonal variation of Br (a) and BrO (b) concentration in the surface air at different latitudes as simulated by the p-TOMCAT model.*

Vertical downscaling of concentration profiles. Evaluation of simulations results against measurements is essential component of the analysis presented below. In majority situations ground base observations, including Hg measurements, are performed at a few meters height from the ground. (For instance, discussed below speciated measurements of Hg at site Waldhof were performed at 5 m height.) On the other hand, model simulated concentrations commonly related to the lowest model layer located at few tens of meters aloft (around 40 m for GLEMOS). This discrepancy complicates comparison of simulated results with observations, particularly, for substances characterized by intensive interaction with the surface.

To improve the evaluation procedure a mechanism reconstructing the vertical profile of a modelled species and scaling the concentration at the model lowest layer down to the measurement height was developed. The process describing interaction of a gas or particulate species with the surface is dry deposition. As the first approximation we expect that dry deposition flux does not change significantly

with time near the surface: Fdry(z) = const. In the model parameterisation the dry deposition flux is presented as a product of the species concentration and dry deposition velocity. The latter is commonly described by the resistance analogy approach:

$$V_d = (R_a + R_b + R_c)^{-1},$$

where $R_a = R_a(z)$ is the aerodynamic resistance as a function of height; R_b is the resistance of the laminar boundary layer; R_c is the surface resistance. With confidence we can expect that the measurement point is located much higher than the laminar boundary layer. Therefore, R_b and R_c can be considered unchangeable. Equating the fluxes at different heights we can express concentration at the measurement height through the simulated concentration at the lowest model layer:

$$C(z) = C^{ref} \frac{R_a(z) + R_b + R_c}{R_a^{ref} + R_b + R_c},$$

where R_a^{ref} and C^{ref} are aerodynamic resistance and simulated concentration at the lowest model layer. The function $R_a(z)$ is calculating using the standard parameterisation applied in the model. The examples of calculated vertical profiles for GOM and PBM are shown in Fig. 2.3. As seen, GOM has a stronger decreasing profile due to its larger dry deposition velocities.

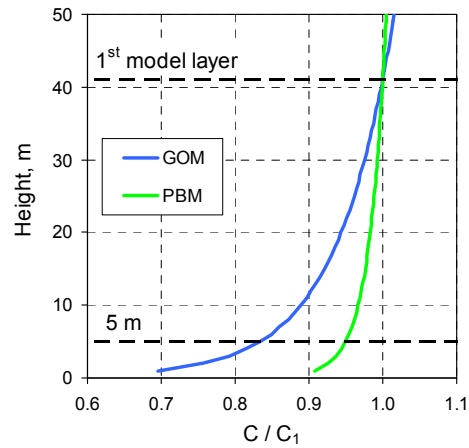

Fig. 2.3. *Vertical profiles of GOM and PBM calculated using the downscaling procedure*

2.2. Simulations program

The updated version of GLEMOS was applied for simulation of short-term observational episodes involving detailed measurements of Hg species at ground monitoring sites, ship-based and aircraft platforms. The aim of the study was evaluation of principal processes of Hg transport and transformations in the atmosphere. For this purpose the model was applied in a number of case studies corresponding to Hg observations in different atmospheric environments:

1. Continental boundary layer CBL (Waldhof monitoring station, Germany, 2009);
2. Upper troposphere and lower stratosphere (CARIBIC project, 2009)
3. Free troposphere and stratospheric intrusions (WAMO project, North America, 2010)
4. Marine boundary layer MBL (RV Urania cruise, Mediterranean Sea, 2012).

In order to evaluate different physical and chemical mechanisms the model performed a number of sensitivity runs with various parameterizations and/or combinations of considered processes. The main focus of the analysis includes evaluation of speciation of Hg anthropogenic emissions; testing the major mechanisms of Hg oxidation in the CBL, MBL, and the upper troposphere and examining the physical state of the oxidation products (gaseous or particulate). Simulation results of the first two case studies (Waldhof and CARIBIC) are presented below along with preliminary analysis. Model simulations for two other case studies are still in progress and their results will be published later along with the results of regional scale modelling.

2.3. Case 1: Waldhof station, 2009

The background EMEP monitoring station Waldhof (DE2) is situated in northern Germany on typical flatland surrounded by forest area with some agriculture and meadows (www.emep.int). No significant built-up areas or industrial facilities are located in the surroundings. Starting from 2009 speciated round-year measurements of Hg have been started at Wladhof with high temporal resolution. Observations of total gaseous mercury (TGM), gaseous oxidized mercury (GOM) and particle-bound mercury (PBM) from this site were utilized to study Hg behaviour in the continental boundary layer (CBL).

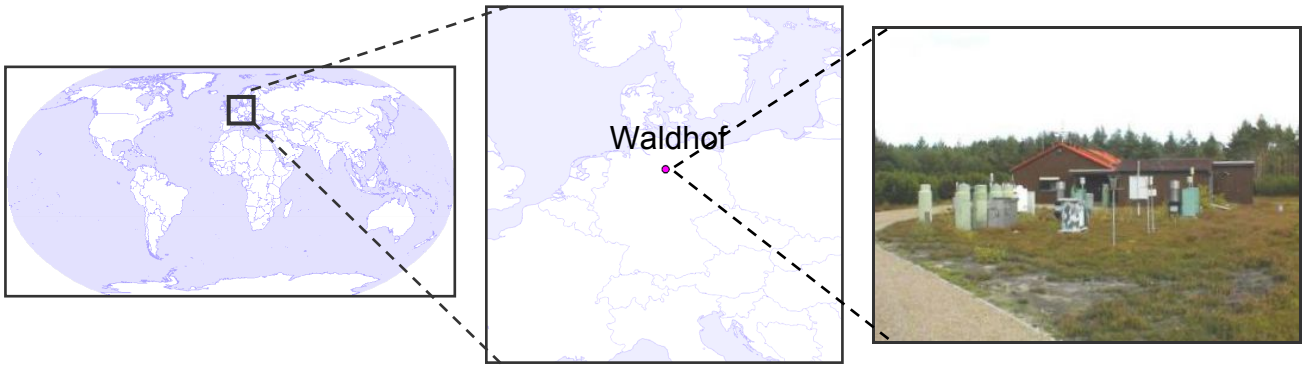

Fig. 2.4. *Location of the EMEP monitoring station Waldhof, Germany (DE2)*

Concentrations of TGM, GOM and PBM observed at Waldhof in 2009 are shown in Fig. 2.5. Temporal resolution of available measurement data is 1 hour for gaseous elemental mercury (GEM) and about 4.5 hour for GOM and PBM. Annual mean concentration of TGM over the whole year dataset is 1.7±0.3 ng/m^3, which is typical for background areas of Europe. Measured GOM concentrations present quite low yearly mean value of 1.6±2.4 pg/m^3. Taking into account short residence time of GOM in the atmosphere, one can suppose photochemical origin of GOM in this remote location. This assumption is also supported by the fact that GOM concentrations are considerably higher during summertime and have pronounced diurnal cycle. Concentrations of PBM are noticeably larger and make up 9.9±11.8 pg/m^3 on average. Temporal variation of PBM has no evident diurnal or seasonal pattern. Therefore, one can expect significant influence of emission sources on PBM concentrations at this site.

The process study mentioned above involves significant number of the model sensitivity runs. To reduce amount of model simulations we restricted our analysis by a shorter time episode 29 March – 20 April 2009 (Fig. 2.5). The main criterion of the selection was absence of precipitation over the monitoring site and surrounding area during considerable period. The focus of this case study is simulation of oxidation chemistry and reproduction of air concentrations of the oxidized Hg species (GOM and PBM). Precipitation scavenging significantly affects air concentration of GOM and PBM. Therefore the choice of a dry period allows excluding the effect of wet scavenging from the consideration and focusing on the processes of emissions, chemical formation and atmospheric transport. During the considered period concentrations of TGM, GOM and PBM were somewhat higher than the yearly averages – 1.92±0.36 ng/m^3, 2.28±2.26 pg/m^3, and 15.7±8.2 pg/m^3, respectively.

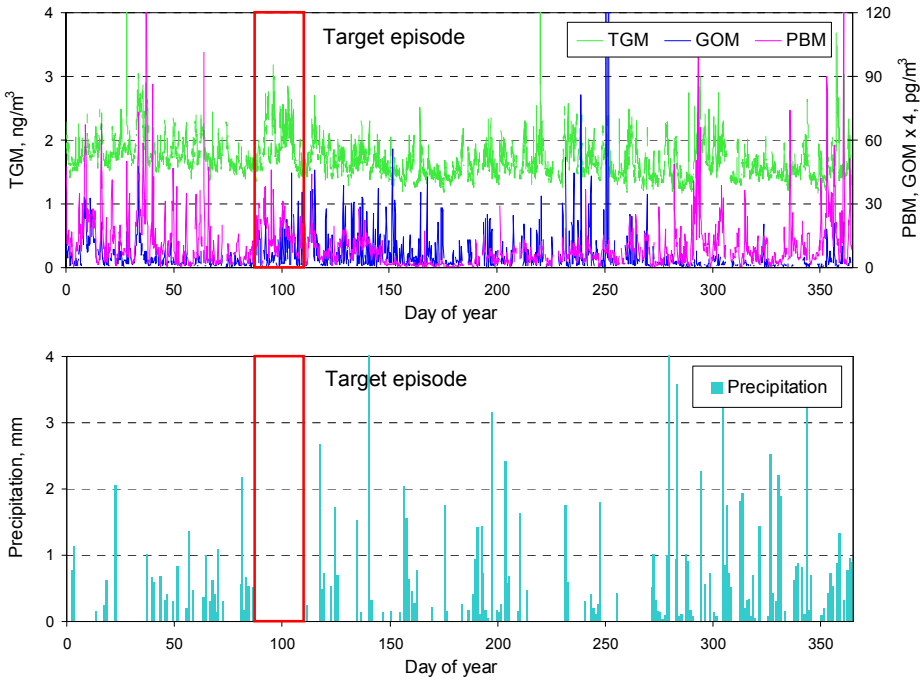

Fig. 2.5. *Observed concentrations of Hg species (a) and precipitation amount (b) at the Waldhof site in 2009. Red rectangle shows the selected simulation episode (29 March – 20 April 2009)*

The simulations procedure was as follows. The model has been run for a spin-up period of 3 years to generate initial conditions (ICs) for the sensitivity runs. After that a series of model runs have been performed for the 2-months period (March-April) with various combinations of chemical mechanisms of Hg oxidation and physical states of the oxidation products. An additional spin-up period (March) was included to bring concentrations of GOM and PBM to the steady state. The list of the sensitivity runs is given in Table 2.2 The base run (Run 1) corresponds to the state-of-the-art configuration of the model. A special model run (Run 1a) has been performed under the same conditions corresponding to the base run but with zeroed ICs for GOM and PBM. It was shown that one month spin up is enough to generate steady state concentrations of short-lived oxidized Hg forms and by the beginning of the target period (29 March) concentrations of GOM and PBM in Runs 1 and 1a become almost identical. Therefore, in all other sensitivity runs ICs for GOM and PBM were zeroed.

Table 2.2. *Parameters of the model sensitivity runs for Case Study 1 (Waldhof)*

Runs	Initial conditions	Anthropogenic Emissions	Oxidation agents	Oxidation products	Comments
1	GEM, GOM, PBM	GEM, GOM, PBM	O_3, OH [(a)]	PBM	Base run
1a	GEM	GEM, GOM, PBM	O_3, OH	PBM	Test of the effect of zero ICs for GOM and PBM
2	GEM	GEM, GOM, PBM	–	–	No oxidation chemistry
3	GEM	GEM	O_3	GOM	Oxidation by O_3, products GOM
4	GEM	GEM	O_3	PBM	Oxidation by O_3, products PBM
5	GEM	GEM	OH	GOM	Oxidation by OH, products GOM
6	GEM	GEM	OH	PBM	Oxidation by OH, products PBM
9	GEM	GEM	Br	GOM	Oxidation by Br, products GOM
10	GEM	GEM	Br	PBM	Oxidation by Br, products PBM

a - OH photochemical activity is redused in the cloud environment according to [*Seigneur et al.*, 2001]

Figure 2.6 shows comparison of observed and simulated TGM concentrations at site Waldhof over the considered period. As seen the model relatively well reproduces both general levels and temporal variation of the observed TGM. Besides, the replacement of chemical mechanisms only slightly alters the simulated TGM over this short period. Given that TGM consists of GEM by more than 98%, it means that only insignificant portion of GEM undergoes *in situ* oxidation by the considered mechanisms. Exceptions are Runs 9 and 10 corresponding to application of Br chemistry. In this case, TGM experiences deeper depletion in some days due to the oxidation chemistry. Keeping in mind that GOM and PBM are more sensitive to the chemical processes, the further analysis is focused on concentrations of the oxidized Hg forms and their comparison with observations.

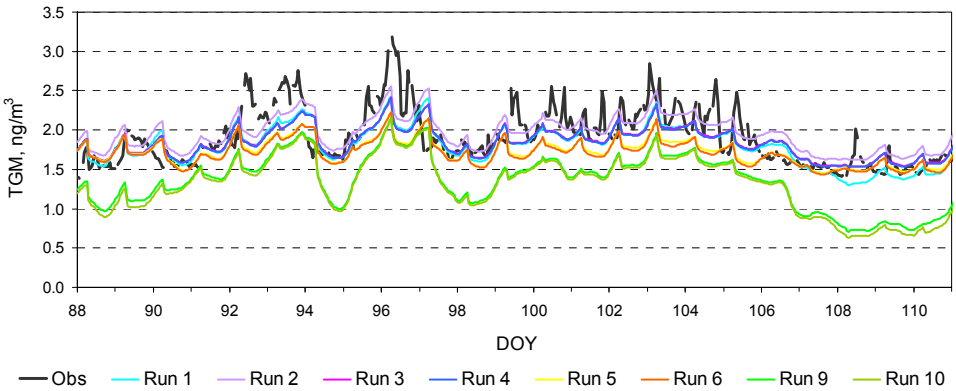

Fig. 2.6. *Comparison of measured and simulated TGM concentration at Walhof during the selected episode (29 March – 21 April 2009)*

Comparison of simulated concentrations of GOM and PBM with observations at site Waldhof over the selected period (29 March – 20 April 2009) is presented below for each of sensitivity runs separately. The time series show concentration variation with original temporal resolution (4.5 hour for measurements and 1 hour for modelling), whereas the scatter plots present comparison of 6-hour concurrent aggregated data. Taking into account that observed and simulated concentrations differ significantly in some cases their values are shown in different scales. The figures present estimated GOM and PBM concentrations both at the lowest model layer (~35 m) and at 5 m height above ground. For all model runs the difference between calculated concentrations at the two above heights is noticeable for GOM and almost negligible for PBM. Summary of the statistics of mode vs. observations comparison for all sensitivity runs is given in Table 2.3.

Base run. The base model run (Run #1) was performed using the current state-of-the-art configuration of GLEMOS. It includes anthropogenic and natural/secondary emissions, full gas-phase and aqueous-phase Hg chemistry, transport and deposition [*Travnikov and Ilyin*, 2009]. The gas-phase chemistry involves oxidation reactions with O_3, OH, Cl_2, Br/BrO (in the polar regions). It should be noted that in the base configuration reactivity of OH is reduced in the cloud environment according to [*Seigneur et al.,* 2004].

As seen from Fig. 2.7 simulated GOM and PBM significantly overestimate observation: by a factor of 5-9 for GOM and by a factor of 3 for PBM on the average. As it was mentioned above the difference between concentration estimates at two different heights is much larger for GOM than for PBM because of greater near-surface concentration gradient of GOM. Along with smaller overestimation PBM results are also characterized by better correlation with observations (Table 2.3). The reasons of the overestimation are analysed in the next sensitivity run (Run #2).

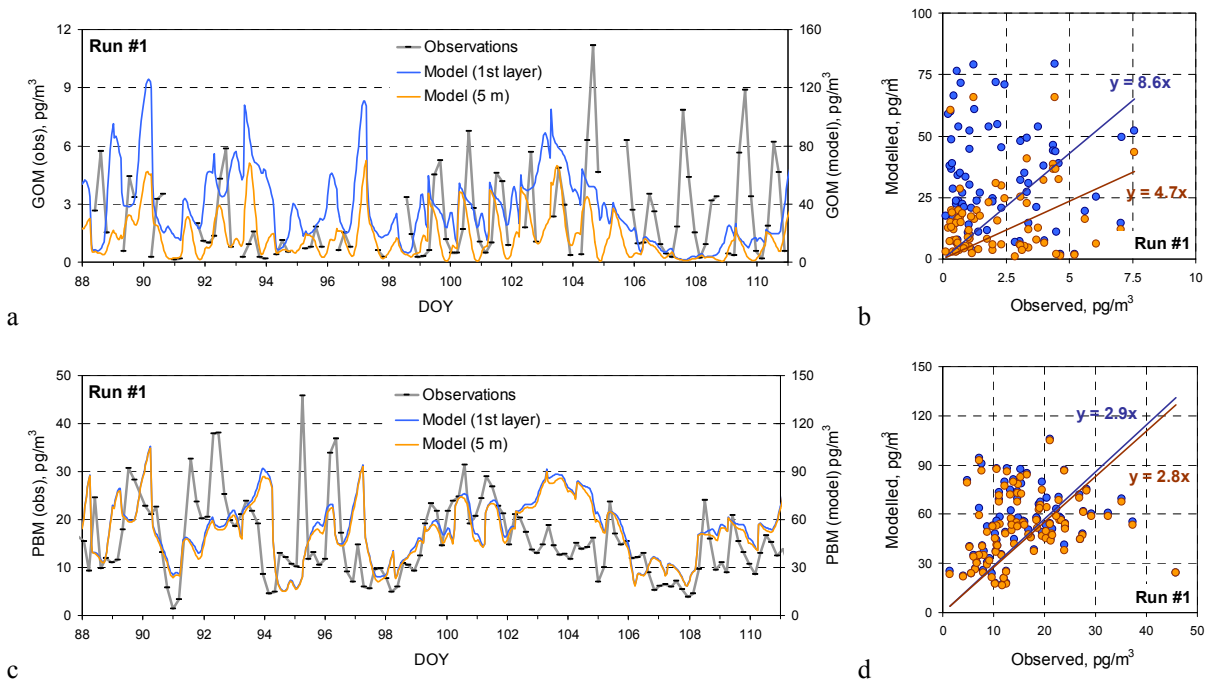

Fig. 2.7. *Comparison of simulated and measured concentration of GOM (a, b) and PBM (c, d) at Walhof during the selected episode (29 March – 20 April 2009) for the sensitivity Run 1. Time series show measured and modeled data with original temporal resolution; scatter plots present comparison of aggregated 6 hourly concentrations.*

No gas-phase oxidation chemistry. In Run #2 no oxidation chemistry was included into the model simulations. In addition, as it was mentioned above, ICs for all sensitivity runs include only GEM but not GOM and PBM. Thus, the oxidized forms enter the atmosphere only from anthropogenic sources. It allows assessing effect of direct anthropogenic emissions on the simulation results. As seen, even in this case we have the same overestimation of observed GOM by a factor of 5-9 (Fig. 2.8). Moreover, the simulated GOM concentrations look almost identical to those in the base run. It means that anthropogenic emission is dominating source of GOM simulated in the base run. Another conclusion is that anthropogenic emissions of GOM are overestimated at least by a factor of 5 in the area influencing observations at Waldhof (Central Europe).

It is interesting to note that GOM estimates at 5 m better correlate with observations than those at 35 m (see Table 2.3) and partly reproduce the diel cycle with minimums at night and maximums at noon. The reason for that is probably variation of local meteorological conditions, in particular, stability of the boundary layer. Dry deposition from shallow nocturnal boundary layer leads to stronger near-surface gradient and lower ground concentrations. The overestimation of observed PBM is smaller than in the base run (factor of 1.6). Since the photochemistry was not included in this run, one can conclude that PBM anthropogenic emissions are also overestimated, at least, by 60%. Thus, a possible reason of the model overestimation of GOM and PBM concentrations is wrong speciation of anthropogenic emissions used in the modelling.

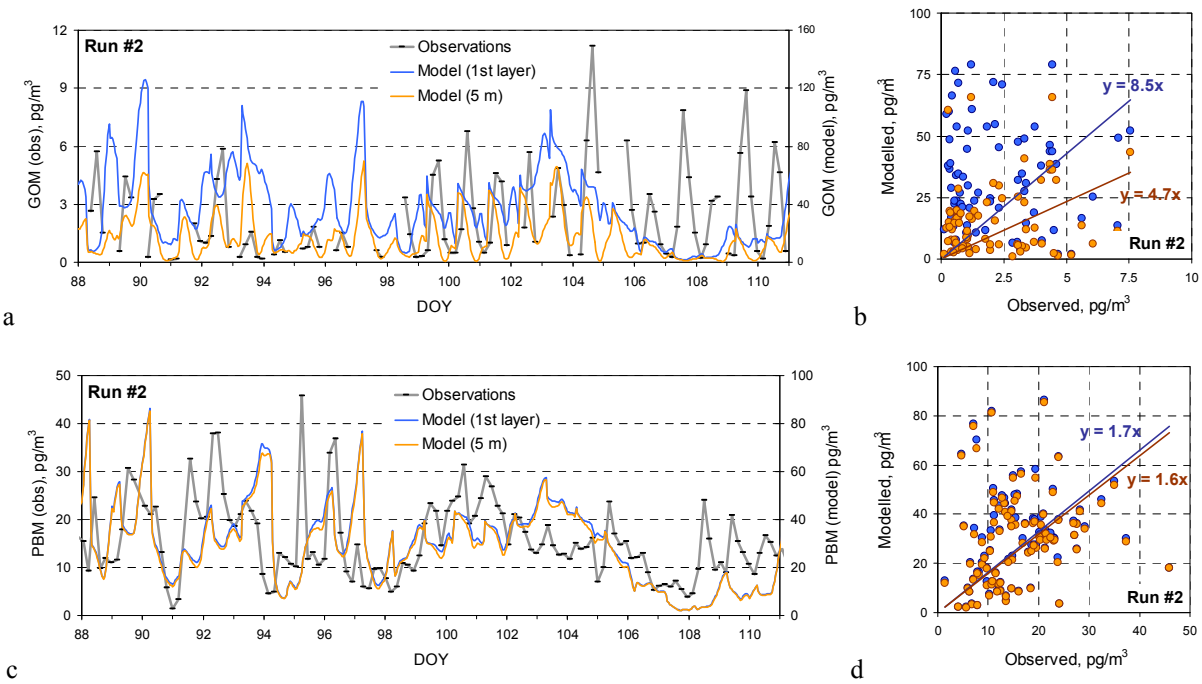

Fig. 2.8. *Comparison of simulated and measured concentration of GOM (a, b) and PBM (c, d) at Walhof during the selected episode (29 March – 20 April 2009) for the sensitivity Run 2. Time series show measured and modeled data with original temporal resolution; scatter plots present comparison of aggregated 6 hourly concentrations.*

$Hg^0 + O_3 \rightarrow$ products (GOM) | no GOM and PBM emissions. In Run #3 as well as in all the following runs no GOM and PBM emissions were included. The major source GOM and PBM in the atmosphere was the gas-phase oxidation of GEM. There was also an indirect minor source due to interaction of the gas-phase species with the aqueous phase of cloud, rain and fog. It is assumed in the model that PBM can be produced from the aqueous Hg species after full evaporation of cloud/rain/fog droplets. Run #3 considers the only chemical mechanism of GEM oxidation through the reaction with O_3. Products of the reaction are treated as GOM. The simulation results are shown in Fig. 2.9. In this case the model successfully reproduces measured GOM concentrations with no overestimation (for the estimates at 5 m height) and significant temporal correlation (r=0.64). Simulated PBM in this case is a product of evaporation of the aqueous phase only and, therefore, it largely underestimates (by a factor of 3) and does not correlate with measurements. We should note that this sort of oxidation reaction can hardly occur in gas phase (with GOM as a product) under realistic atmospheric conditions as it was shown by a number of theoretical studies [*Shepler and Peterson,* 2003; *Tossell,* 2003; *Calvert and Lindberg,* 2005]. Nevertheless, it demonstrates possibility to explain the observed behaviour of GOM with a photochemical mechanism.

$Hg^0 + O_3 \rightarrow$ products (PBM) | no GOM and PBM emissions. Conditions of Run #4 are the same as those for Run #3 except for the product of the oxidation reaction, which is treated as PBM in this case. As shown in Fig. 2.10, GOM concentrations in this run are extremely low but non-zero, because of gas exchange with the aqueous phase. Interestingly, the correlation is significant (r=0.36) even in this case indicating oxidation of Hg in the aqueous phase that experience similar diel cycle. Simulated PBM concentrations slightly (by 20%) underestimate the measurements. The model captures some observed peaks but the model-to-measurement correlation is generally lower than in Run #2. It means that PBM levels at this site are partly determined by direct anthropogenic emissions and partly by photo-oxidation with larger contribution of the former factor.

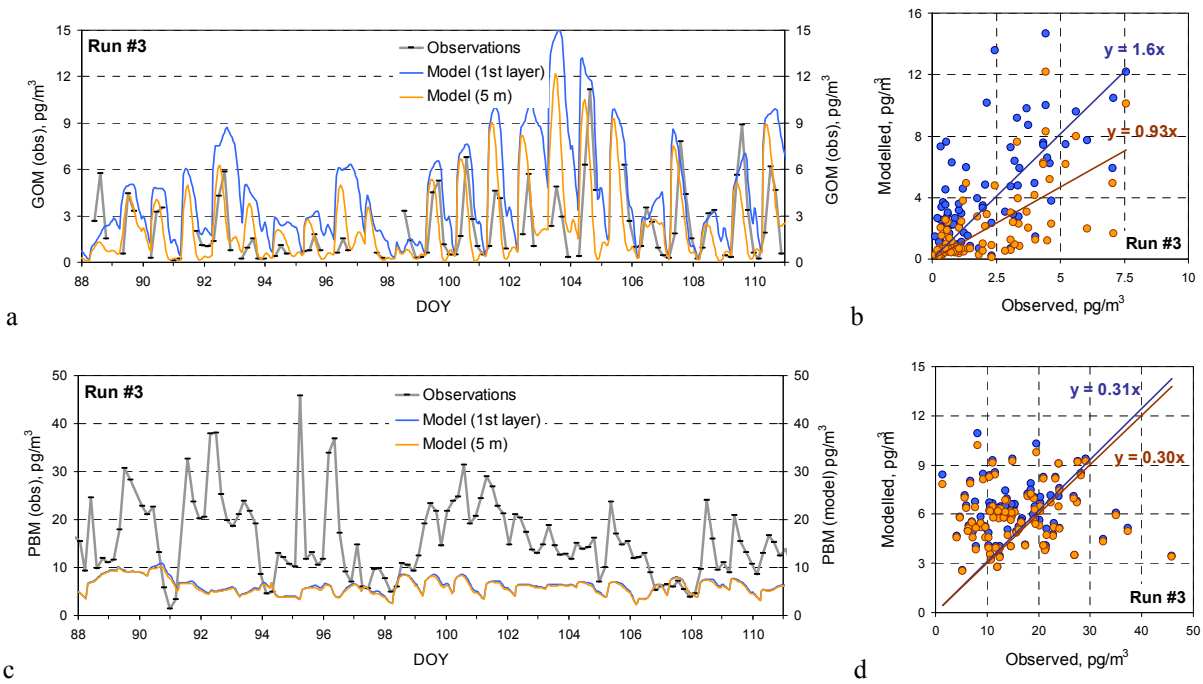

Fig. 2.9. *Comparison of simulated and measured concentration of GOM (a, b) and PBM (c, d) at Walhof during the selected episode (29 March – 20 April 2009) for the sensitivity Run 3. Time series show measured and modeled data with original temporal resolution; scatter plots present comparison of aggregated 6 hourly concentrations.*

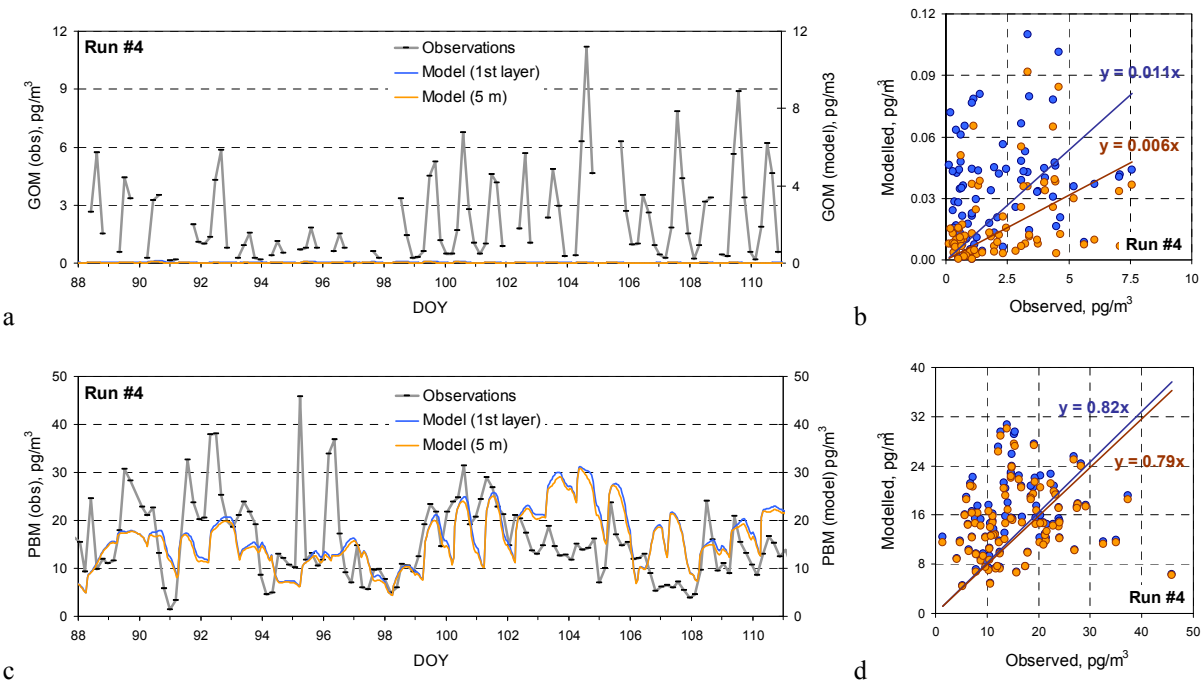

Fig. 2.10. *Comparison of simulated and measured concentration of GOM (a, b) and PBM (c, d) at Walhof during the selected episode (29 March – 20 April 2009) for the sensitivity Run 4. Time series show measured and modeled data with original temporal resolution; scatter plots present comparison of aggregated 6 hourly concentrations.*

Hg^0 + OH → products (GOM) | no GOM and PBM emissions. In Run #5 the only process responsible for the formation of GOM is the GEM oxidation reaction with OH radical. Nevertheless, application of this mechanism alone leads to 3-5-fold overestimation of the measurements (Fig. 2.11). However, it should be mentioned that simulated GOM concentrations also well correlate with observed levels (r=0.6) demonstrating the temporal pattern similar to the pattern obtained due to reaction with O3 (Run #3). It is explained by similar diel variation of both photo-oxidants in this region. Overestimated GOM concentrations led to formation of significant PBM levels produced from evaporation of the aqueous Hg phase. The simulated PBM concentrations are only slightly below the observations but poorly correlate with them. It means that contribution of this process is also largely overestimated by the model in this particular case.

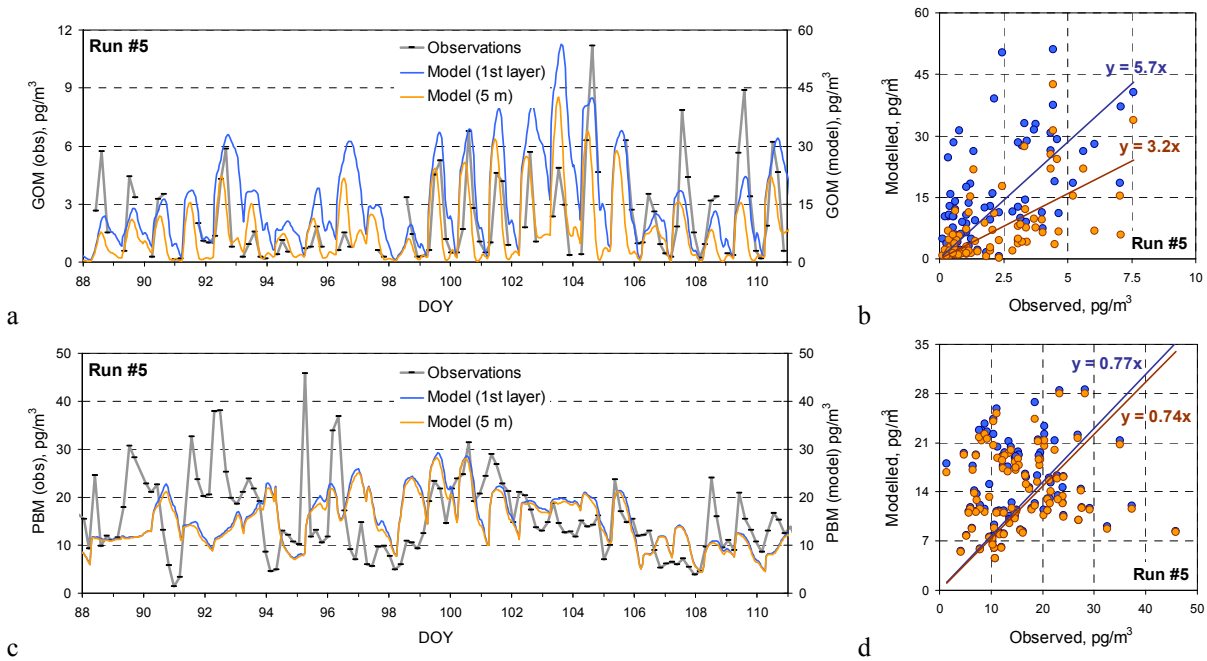

Fig. 2.11. *Comparison of simulated and measured concentration of GOM (a, b) and PBM (c, d) at Walhof during the selected episode (29 March – 20 April 2009) for the sensitivity Run 5. Time series show measured and modeled data with original temporal resolution; scatter plots present comparison of aggregated 6 hourly concentrations.*

Hg^0 + OH → products (PBM) | no GOM and PBM emissions. Oxidation of GEM in reaction with OH radical was simulated in Run #6 with the reaction products treated as PBM. Simulated GOM concentrations are negligible (Fig. 2.12) but slightly correlated with measurements due to oxidation in the aqueous phase. PBM levels are overestimated by the model by factor of 2.5. The model captured a number of observed peaks; however, the correlation over the whole period is low. As in a similar case of the reaction with O_3 it might imply prevailing influence of other factors, such as direct anthropogenic emissions.

Hg^0 + Br → products (GOM) | no GOM and PBM emissions. GEM oxidation by atomic Br was studied in Runs #9 and #10. In Run #9 products of both reactions were treated as GOM. Simulated GOM concentrations relatively well reproduce temporal variation of observations (r=0.57), however, overestimate the observed values by a factor of 2.5-4 on average (Fig. 2.13). The overestimation is larger in the beginning and by the end of the period, when the model predicts very high GOM concentration as a result of more intensive in situ oxidation of GEM. The reason of the high oxidation rate during this time relates to high Br concentration and lower air temperature. This effect is even more pronounced for PBM. Concentrations of secondary PBM formed from the aqueous phase are comparable with the observed PBM levels in the middle of the period but much larger those in the

beginning and by the end of it. Given that the simulated extreme PBM concentrations are higher than GOM concentrations, the particulate species or of the aqueous phase should originate elsewhere and then transported to the measurement site. Thus, application of the Br chemistry allows reproducing temporal variation of GOM over the major part of the period but leads to large episodic overestimations.

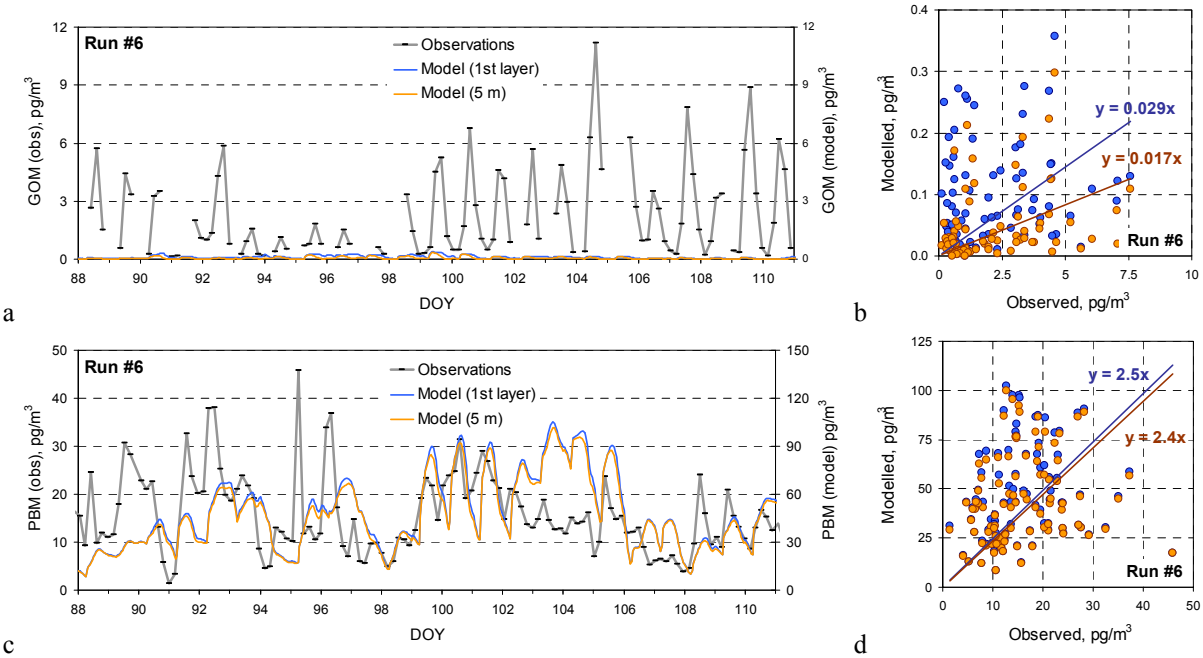

Fig. 2.12. *Comparison of simulated and measured concentration of GOM (a, b) and PBM (c, d) at Walhof during the selected episode (29 March – 20 April 2009) for the sensitivity Run 6. Time series show measured and modeled data with original temporal resolution; scatter plots present comparison of aggregated 6 hourly concentrations.*

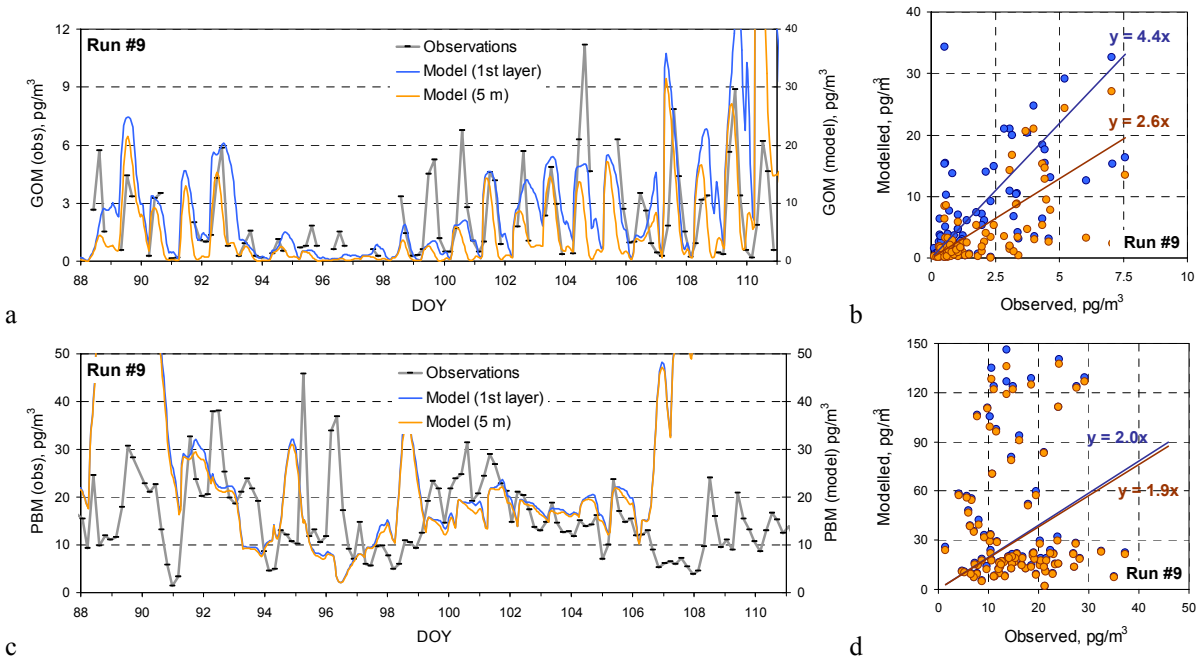

Fig. 2.13. *Comparison of simulated and measured concentration of GOM (a, b) and PBM (c, d) at Walhof during the selected episode (29 March – 20 April 2009) for the sensitivity Run 9. Time series show measured and modeled data with original temporal resolution; scatter plots present comparison of aggregated 6 hourly concentrations.*

Hg^0 + Br → products (PBM) | no GOM and PBM emissions. Run #10 also studies Hg oxidation by Br but treats the reaction products as PBM (Fig. 2.14). No wonder that simulated GOM concentrations are negligible but somewhat correlated with observations (r=0.37). The only source of GOM in this case was photo-oxidation of Hg^0 in the aqueous phase evasion to the air. Concentrations of PBM as a product of the oxidation reaction are much higher and overestimate the observed values by a factor of 3.5 on average. However, the overestimation differs for different parts of the period as it was mentioned for Run #9. It does not exceed a factor of 1.6 in the middle of the period and is much higher in the beginning and by the end of it. The large overestimation at the ends of the period results from artificially high oxidation because of elevated concentrations of Br in these periods and/or overpredicted oxidation kinetics.

Summary of the statistical parameters (the linear regression coefficient and the Pearson's correlation coefficient) of the model-to-observation comparison for all model runs is given in Table 2.3. As seen, the highest temporal correlation (shown in bold) of simulated and measured GOM concentrations is obtained for Runs #3, #5, #9 corresponding to GEM oxidation by O_3, OH radical and atomic Br. The correlation coefficients for these runs are much higher than that for Run #2, when the only source of GEM is anthropogenic emissions. Thus, GOM concentration at this background site is rather affected by atmospheric chemistry than by direct emissions. In the case when O_3 is considered as the only GEM oxidant the linear regression is close to identity (at the 5 m height) meaning absence of any overestimation, whereas in the two latter cases the model overestimates the observations roughly by a factor of 3. One should keep in mind that no GEM emissions were utilized in these runs. Therefore, each of the considered oxidation mechanisms taken alone leads to overestimation of measured GOM concentration when the reaction products are treated as GOM. The reasons of the overestimation include possibility of gas-particle partitioning of the oxidation products, overstating of the oxidation reaction rates or existence of a gas-phase reduction mechanisms transforming GOM back to GEM. There is also possibility of the model underprediction of GOM removal processes (mostly, dry deposition).

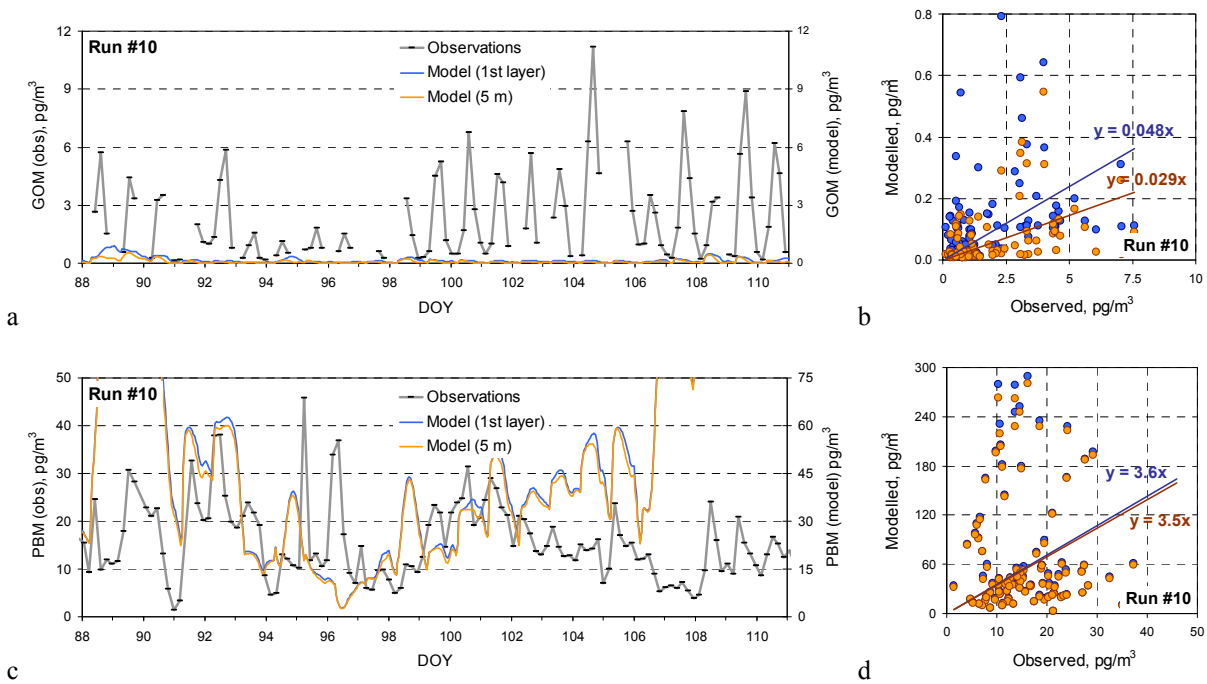

Fig. 2.14. Comparison of simulated and measured concentration of GOM (a, b) and PBM (c, d) at Walhof during the selected episode (29 March – 20 April 2009) for the sensitivity Run 10. Time series show measured and modeled data with original temporal resolution; scatter plots present comparison of aggregated 6 hourly concentrations.

In contrast with GOM, correlation of simulated PBM concentrations with observations is higher for Run #2, which considers anthropogenic emissions as the only source of GOM and PBM. It implies prevailing contribution of emissions to PBM concentration at the considered site. However, as follows from the results of Runs #4, #6, #10, contribution of the oxidation chemistry can be also significant. Application of the oxidation mechanisms with OH and Br leads to large overestimation of measured PBM concentrations by the model accompanied by poor correlation. Additional analysis is needed to distinguish between the effects of emissions and chemistry.

Table 2.3. *Summary of the statistics of model vs. observations comparison for different sensitivity runs (6-hourly data). Statistical parameters are presented for both the first model layer and 5 m height (divided by slash).*

Run #	GOM		PBM	
	Linear regression	Pearson's correlation	Linear regression	Pearson's correlation
1	8.6 / 4.7	-0.07 / 0.18	2.9 / 2.8	**0.22 / 0.23**
2	8.5 / 4.7	-0.07 / 0.17	1.7 / 1.6	**0.21 / 0.21**
3	1.6 / 0.93	**0.65 / 0.64**	0.31 / 0.3	0.05 / 0.06
4	0.011 / 0.006	0.23 / 0.36	0.82 / 0.79	0.14 / 0.14
5	5.7 / 3.2	**0.59 / 0.6**	0.77 / 0.74	0.08 / 0.09
6	0.029 / 0.017	0.14 / 0.28	2.5 / 2.4	0.16 / 0.17
9	4.4 / 2.6	**0.54 / 0.57**	2.0/ 1.9	-0.02 / -0.02
10	0.048 / 0.029	0.26 / 0.37	3.6 / 3.5	-0.04 / -0.03

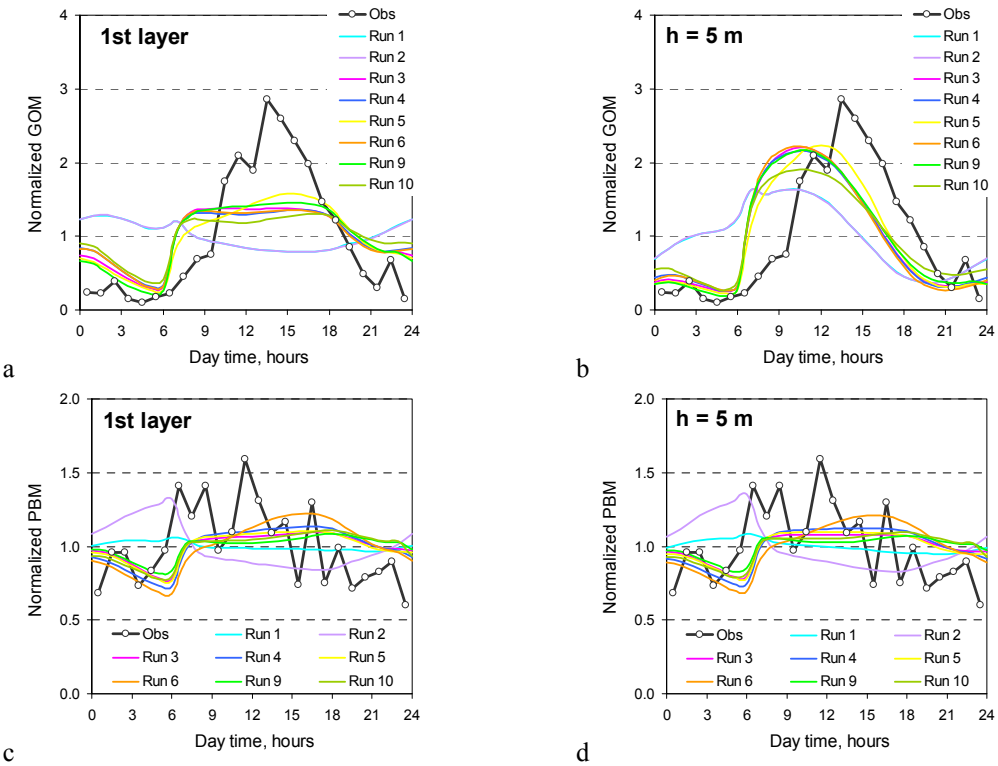

Fig. 2.15. *Diurnal variation of normalized GOM (a, b) and PBM (c, d) concentrations at Waldhof averaged over the period 29 March – 20 April.*

The model ability to reproduce diurnal cycle of GOM and PBM concentrations is additionally considered. Figure 2.15 shows diurnal variation of normalized GOM and PBM concentrations at

Waldhof both measured and simulated in all sensitivity runs. Observed GOM experiences significant changes during daytime with maximum at afternoon and minimum at night indicating evident effect of photochemistry. The model generally reproduces the diurnal cycle in all runs involving oxidation chemistry (Runs 3–10). The amplitude of variation is more pronounced near the surface (5 m) than aloft at the lowest model layer. It is remarkable that the shape of GOM diurnal variation is very similar for all the runs. The maximum of simulated concentration is shifted by a few hours forward in time, probably, due to rough resolution of input data on reactants concentrations (6 hourly). It should be noted that simulated GOM concentrations, which dominated by anthropogenic emissions (Runs #1 and #2), poorly correlate with the observed diurnal cycle.

The diurnal variation of observed PBM concentration is less pronounced. Concentrations are somewhat higher during daytime than at night. Modelled PBM concentrations demonstrate relatively stable levels. It is remarkable that the sensitivity run driven by anthropogenic emissions (Run #2) evidently anti-correlate with runs considering oxidation chemistry. The latter (Runs #3-10) predict moderate minimum of PBM concentration in the early morning and a weak maximum in the afternoon, whereas the former (Run #2) demonstrates the opposite variation with a maximum in the morning and minimum in the afternoon. As a result, the base run (Run #1) including both emissions and oxidation chemistry shows absence of any significant diurnal variation.

2.4. Case 2: CARIBIC

Total gaseous Hg (TGM) was measured in the upper troposphere and lower stratosphere as a part of the CARIBIC project (Civil Aircraft for the Regular Investigation of the atmosphere Based on an Instrument Container). The project is aimed at study and monitor of important chemical and physical processes in the atmosphere. Detailed and extensive measurements are made during long distance flights using automated scientific apparatus encased in an airfreight container onboard a passenger Lufthansa aircrafts. Along with gaseous mercury many other substances (CO, O_3, NO, NO_y, CO_2 etc.) and aerosol are measured during a flight. Some details of Hg measurements within CARIBIC are available in [*Slemr et al.,* 2009].

Four CARIBIC flights were chosen for the analysis directed to different parts of the northern and southern hemispheres in 2009:

Flight 1: Frankfurt – Caracas – Frankfurt (22-23 Apr 2009)

Flight 2: Frankfurt – Vancouver – Frankfurt (23-24 Apr 2009)

Flight 3: Frankfurt – Osaka – Frankfurt (27-28 May 2009)

Flight 4: Frankfurt – Cape Town – Frankfurt (27-29 Oct 2009)

The flight tracks and TGM concentrations measured during the flights are shown in Figure 2.16. The characteristic feature of the TGM measurements are very low values (below 0.6 ng/m^3) observed over long distances in most CARIBIC flights (e.g. Flights 1-3). These depletions of TGM characterise stratospheric parts of the flights and reflect deep oxidation of GEM in the lower stratosphere and association of the reaction products with particulate phase [*Slemr et al.,* 2009].

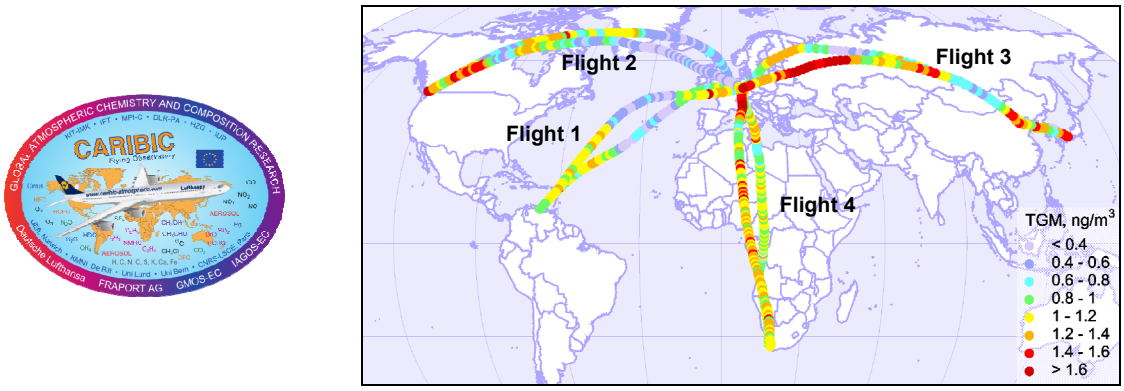

Fig. 2.16. *Flight tracks and observed concentrations of TGM during the selected CARIBIC flights in 2009*

The simulation procedure was similar to that in Case 1. The 3-year model spin-up was performed to generate initial concentrations of GEM, GOM and PBM for the sensitivity runs. Details of the simulations program are given in Table 2.4. One-year sensitivity runs were performed with selected oxidation mechanisms and physical phase of the oxidation products. Initial concentrations and anthropogenic emissions of all three Hg forms are utilized in all model runs. Hourly 3-D model output was used to reconstruct TGM concentrations along the flight tracks.

Table 2.4. *Parameters of the model sensitivity runs for Case 2 (CARIBIC)*

Runs	Initial conditions	Anthropogenic Emissions	Oxidation agents	Oxidation products	Comments
1	GEM, GOM, PBM	GEM, GOM, PBM	O_3, OH [(a)]	PBM	Base run
3	GEM, GOM, PBM	GEM, GOM, PBM	O_3	GOM	Oxidation by O_3, products GOM
4	GEM, GOM, PBM	GEM, GOM, PBM	O_3	PBM	Oxidation by O_3, products PBM
5	GEM, GOM, PBM	GEM, GOM, PBM	OH	GOM	Oxidation by OH, products GOM
6	GEM, GOM, PBM	GEM, GOM, PBM	OH	PBM	Oxidation by OH, products PBM
9	GEM, GOM, PBM	GEM, GOM, PBM	Br	GOM	Oxidation by Br, products GOM
10	GEM, GOM, PBM	GEM, GOM, PBM	Br	PBM	Oxidation by Br, products PBM

[(a)] OH photochemical activity is redused in the cloud environment according to (*Seigneur et al.*, 2001)

Description of the simulation results for selected CARIBIC flights is given below. Each flight is presented by comparison of time series of measured and simulated TGM concentrations and supported by a map of the flight track superimposed on spatial distribution of potential vorticity at 250 hPa isobaric surface (which roughly corresponds to the flight altitude). The latter taken from the KNMI website supported by Dr. Peter van Velthoven (http://www.knmi.nl/samenw/campaign_support/CARIBIC/index.html) and is aimed to identify the flight sections related to the stratosphere and troposphere. In particular, coloured areas in Figs. 2.17 – 2.20 show locations where the isobaric surface is intersected by the tropopause and stratosphere (potential vorticity is above 2 PVU). Uncoloured areas correspond to the troposphere, respectively.

It should be noted that global average levels of TGM in the free troposphere corresponding to different oxidation mechanisms depend to significant extend on the overall balance between GEM input (emissions) and removal (oxidation and deposition). It is possible to obtain the same global TGM averages corresponding to different chemical mechanisms by varying global Hg emissions. Taking

into account high uncertainty of available Hg emission inventories, first of all, from natural and secondary sources, the following analysis is mostly focused on temporal correlation of simulated and observed TGM concentrations. The Pearson's correlation coefficients for all the flights are summarised in Table 2.5 below.

Flight 1: Frankfurt – Caracas – Frankfurt (22-23 April 2009). The first flight came from Europe to South America over the Atlantic (Fig. 2.17). The stratospheric section in the middle of the flight is characterised by drop of measured TGM concentrations below 0.7 ng/m^3. The model catches the stratospheric decrease of TGM in most of the sensitivity runs. However, the depletion is not as deep as it was measured onboard. In general, the chemical mechanisms provide similar variation of TGM during the flight. The base run (Run #1) along with Hg oxidation by O_3 (Runs #3, #4) relatively well reproduce tropospheric concentrations but overpredict concentrations in the stratosphere. Oxidation by OH radical (Runs #5, #6) leads to underestimation of TGM levels in troposphere and fails in reproduction of the troposphere/stratosphere gradient. The Br chemistry (Runs #9, #10) provides intermediate results. As it follows from Table 2.5 the correlation is the highest for the runs with oxidation by O_3 (r=0.7) and the lowest for the OH chemistry (r=0.18).

In the return flight the stratospheric section is shorter and corresponds to the plane path through the narrow plume of the stratospheric intrusion (see Fig. 2.17, lower panels). The model fails reproducing this fine effect, probably, due to low resolution (6 hours) of meteorological input. The poor agreement is clearly indicated in the low correlation coefficients obtained for this flight (Table 2.5; from r=-0.4 to r=0.4)

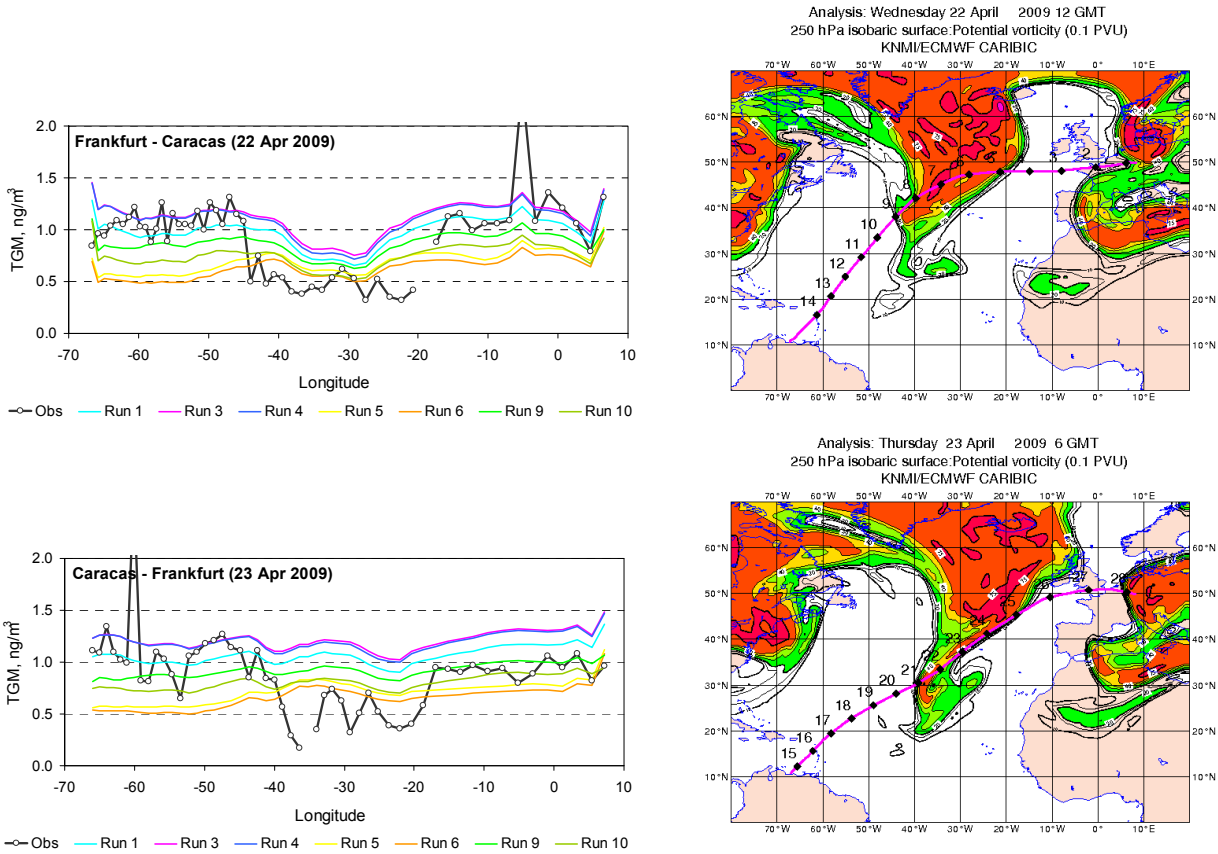

Fig. 2.17. *Comparison of simulated and measured TGM concentration (left column) during the CARIBIC flights Frankfurt-Caracas on 22 April 2009 (upper) and flights Caracas-Frankfurt on 23 April 2009 (lower). The right column shows tracks of the flight along with spatial distribution of potential vorticity at the 250 hPa isobaric surface. Coloured areas at the figure highlight locations of the surface intersection with the tropopause and stratosphere*

Flight 2: Frankfurt – Vancouver – Frankfurt (23-24 July 2009). The spatial variation pattern of the stratosphere boundary height was more complicated during the Flight 2 to Vancouver (Fig. 2.18, right hand panels). The first half of the flight (from 10°E to 40°W) came through the stratosphere. After that the tropospheric and stratospheric sections changed each other with the last stratospheric intrusion occurred just over the landing point. This pattern is clearly reflected in variation of TGM concentration measured onboard (Fig. 2.18, left hand panels). The TGM variation was smoothed somewhat during the return flight but general pattern remained the same. The model generally follows the observed variation of TGM. Temporal correlation is relatively high for all model runs varying from around r=0.7 for the direct flight up to r=0.86 for the return flight (Table 2.5). The highest correlation was obtained for sensitivity runs with Hg oxidation by atomic Br.

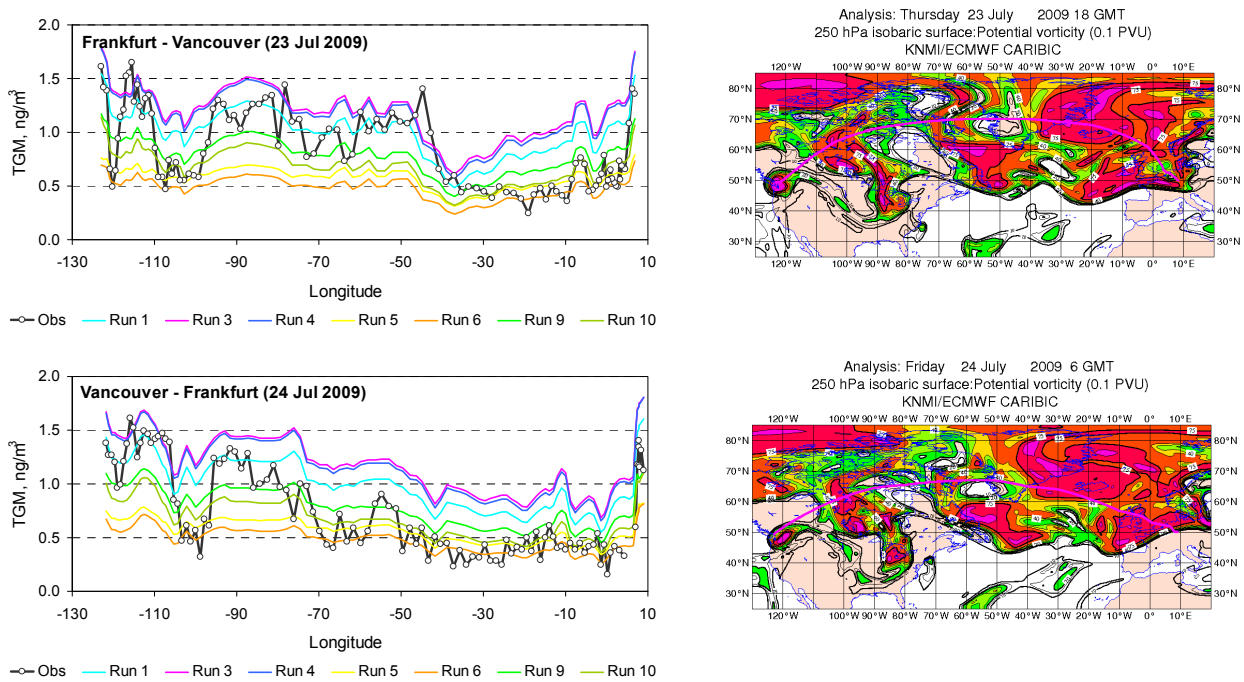

Fig. 2.18. *Comparison of simulated and measured TGM concentration (left column) during the CARIBIC flights Frankfurt-Vancouver on 23 July 2009 (upper) and flights Vancouver-Frankfurt on 24 July 2009 (lower). The right column shows tracks of the flight along with spatial distribution of potential vorticity at the 250 hPa isobaric surface. Coloured areas at the figure highlight locations of the surface intersection with the tropopause and stratosphere*

Flight 3: Frankfurt – Osaka – Frankfurt (27-28 May 2009). The Flight 3 to Osaka over the whole Eurasia also includes a number of tropospheric and stratospheric sections with TGM concentrations dropping down to 0.2 ng/m^3. The model successfully reproduces measured TGM variation during the direct flight (Fig. 2.19; upper panels). Three tropospheric and four stratospheric sections are clearly seen in the simulated TGM time series for all the sensitivity runs. However, the model underpredicts TGM depletion in the stratosphere. The highest model-to-measurement correlation was obtained for sensitivity runs governed by the ozone chemistry (r=0.79), while the lowest correlation was for the runs with the OH oxidation mechanism (r=0.64).

The temporal correlation is significantly lower for the return flight, since the model failed reproducing relatively high TGM concentrations (up to 2 ng/m^3) over the European part of Russia. The reasons for that include uncertainties in reproduction of the stratosphere boundary height or the effect of unaccounted emission sources in this region.

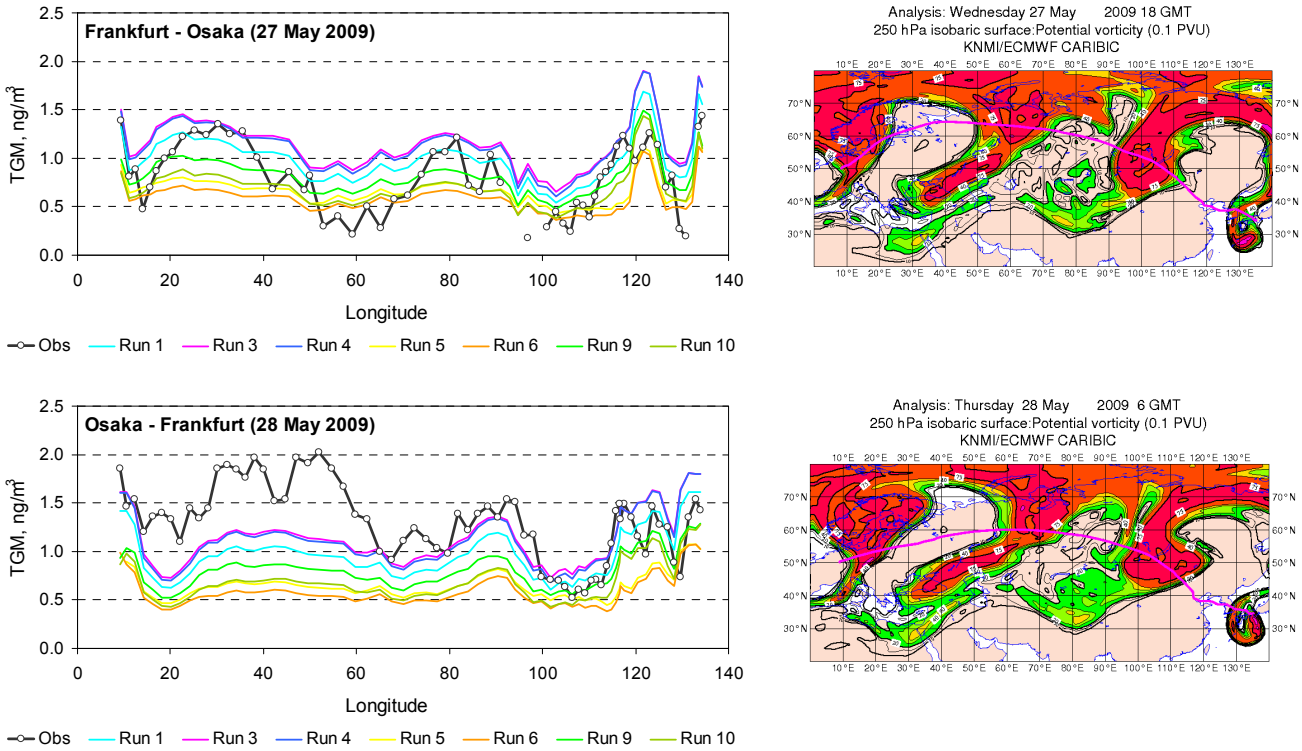

Fig. 2.19. *Comparison of simulated and measured TGM concentration (left column) during the CARIBIC flights Frankfurt-Osaka on 27 May 2009 (upper) and flights Osaka-Frankfurt on 28 May 2009 (lower). The right column shows tracks of the flight along with spatial distribution of potential vorticity at the 250 hPa isobaric surface. Coloured areas at the figure highlight locations of the surface intersection with the tropopause and stratosphere*

Flight 4: Frankfurt – Cape Town – Frankfurt (27-29 October 2009). The Flight 4 to Cape Town passed mainly through the troposphere (Fig. 2.20). Therefore, there were no significant variations of TGM concentrations measured onboard both direct and return flights. The observed time series do not reveal any noticeable gradient of upper tropospheric TGM concentration between the southern and northern hemispheres. In contrast, the model predicts more significant south-to-north increase of TGM concentration. The overall correlation is relatively poor for the direct flight for all the sensitivity runs (r=0.14–0.28). The return flight came through short stratospheric sections over the northern Africa and Europe accompanied by a moderate decrease of TGM concentration (Fig. 2.20, lower panels). The model catches these concentration falls and the model-to-measurement correlation is higher for this flight (up to r=0.48). Similar to other flights, the highest correlation is obtained for the sensitivity runs with Hg oxidation by O_3; it is somewhat lower for the chemistry with atomic Br; and the correlation poor for the reaction with OH radical. It should be noted that the deviation between TGM levels simulated in different sensitivity runs is larger in this case in comparison with other flights. It indicates the fact that the model is not in the steady state for different chemical mechanisms when starting from the same initial conditions. Therefore, more extensive model spin-up is required for each sensitivity run to reach steady-state concentrations in the upper troposphere and the lower stratosphere.

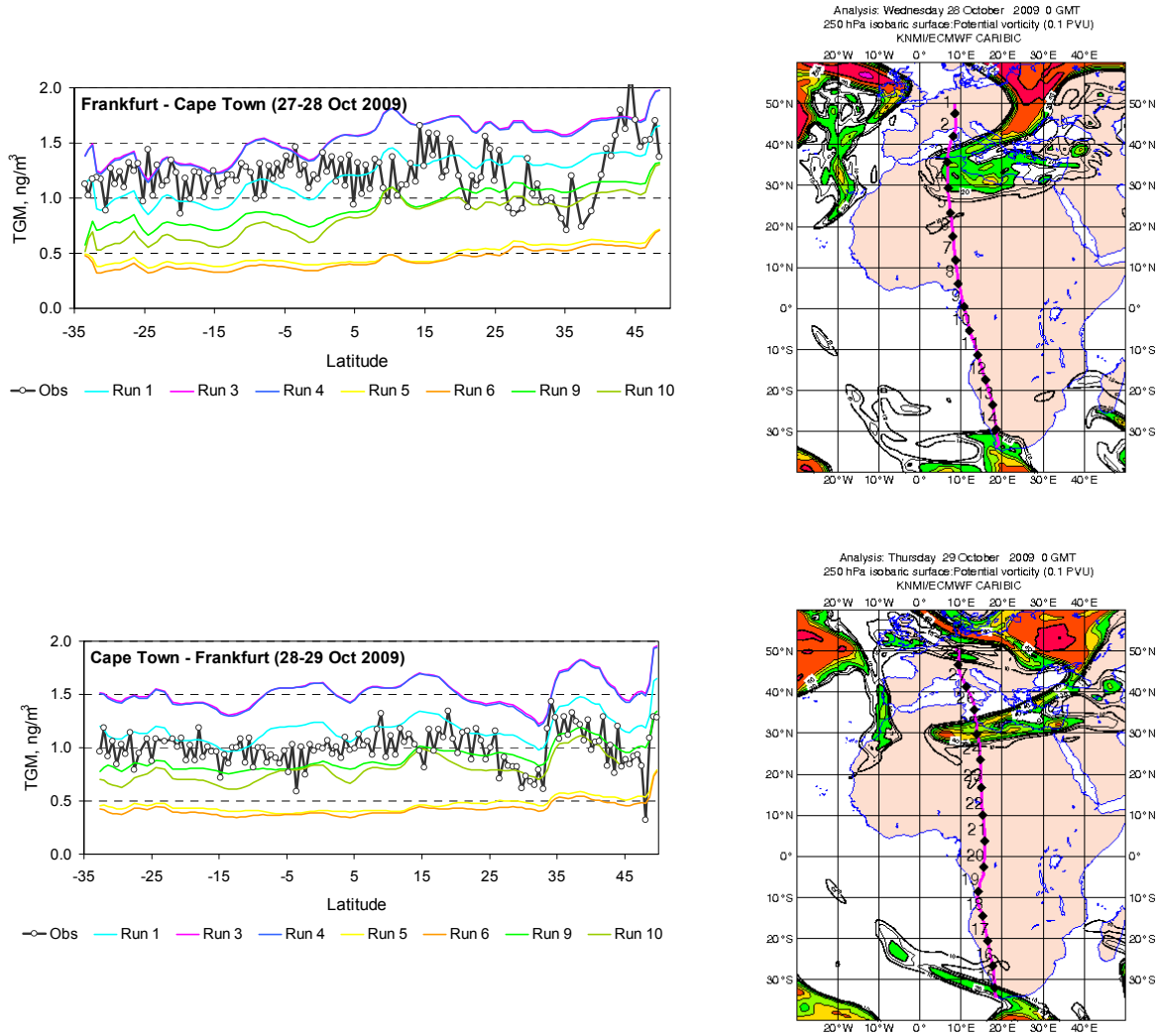

Fig. 2.20. *Comparison of simulated and measured TGM concentration (left column) during the CARIBIC flights Frankfurt-Cape Town on 27-28 October 2009 (upper) and flights Cape Town-Frankfurt on 28-29 October 2009 (lower). The right column shows tracks of the flight along with spatial distribution of potential vorticity at the 250 hPa isobaric surface. Coloured areas at the figure highlight locations of the surface intersection with the tropopause and stratosphere*

Summary of the correlation statistics between the model and observations for all sensitivity runs is given in Table 2.5. As it was mentioned above we do not take into account general underestimation or overestimation of observed levels in different runs since all the run started from the same initial conditions and utilized the same emissions data. On the other hand, more or less oxidative atmospheric conditions can be balanced by higher or lower emission fluxes (e.g. natural or secondary) to obtain realistic levels of TGM in the atmosphere. Evaluation global Hg emission fluxes required to balance different chemical mechanisms in the atmosphere needs additional analysis.

As seen in the table, the highest correlation in the most flights was obtained for the runs governed by the O_3 chemistry. Only slightly lower correlation characterises the simulations with Hg oxidation by atomic Br, whereas application of the OH chemistry commonly produces poorer correlation between the model and observations. Temporal variability of the observed time series of TGM concentration is largely determined by the plane movement between the troposphere and the stratosphere. Therefore,

vertical distributions of the major reactants (O3, OH and Br) defining Hg oxidation in the upper troposphere and lower stratosphere have a primary influence on analysed model-to-measurement comparison. In particular, it means that utilized O3 and Br vertical profiles better reproduce Hg oxidation chemistry in this part of the atmosphere than the vertical distribution of OH. It should be mentioned that the OH reaction kinetics applied in the model does not include temperature dependence of the reaction rate. It could also result in poorer agreement with observations.

Table 2.5. *Pearson's correlation coefficients of the model-to-observation comparison for all sensitivity runs.*

Flight	Direction	Run #1	Run #3	Run #4	Run #5	Run #6	Run #9	Run #10
1	Frankfurt – Caracas	0.65	0.69	**0.70**	0.17	0.18	0.62	0.54
	Caracas – Frankfurt	0.17	0.35	**0.40**	-0.40	-0.37	-0.06	-0.07
2	Frankfurt – Vancouver	0.69	0.69	0.69	0.66	0.69	0.69	**0.71**
	Vancouver – Frankfurt	0.84	0.85	0.85	0.83	0.82	0.86	**0.86**
3	Frankfurt – Osaka	0.77	**0.79**	**0.79**	0.64	0.64	0.74	0.71
	Osaka – Frankfurt	**0.41**	**0.41**	**0.41**	0.35	0.32	0.40	0.33
4	Frankfurt – Cape Town	0.25	**0.28**	**0.28**	0.14	0.18	0.22	0.26
	Cape Town – Frankfurt	0.45	**0.47**	**0.48**	0.26	0.32	0.37	0.43

2.5. Concluding remarks

Presented above sensitivity analysis allows drawing some preliminary conclusions on applicability of different chemical mechanisms for simulation of Hg dynamics in the continental boundary layer (CBL) and under the upper troposphere/lower stratosphere (UT/LS) conditions:

Continental boundary layer (Waldhof)

- Anthropogenic emissions of GOM and PBM are overestimated, at least, by factors of 5 and 1.6, respectively, in the considered area (Central Europe). It could be connected with wrong speciation of available emissions estimates or with possible in-plum reduction of oxidized Hg.
- GOM concentration in CBL is rather affected by atmospheric chemistry than by direct emissions. In contrast, anthropogenic emissions largely contribute to PBM ambient levels.
- Each of the considered oxidation mechanisms (O_3, OH, Br) reproduces diurnal variation of GOM but, even taken alone, leads to large overestimation of measurements, when the reaction products are treated as GOM. It implies existence of gas-particle partitioning.
- Application of each oxidation mechanisms without contribution of emissions leads to poor temporal correlation of simulated PBM with observations. Besides, oxidation by OH and Br results in large overestimation of measured PBM concentrations.

Upper troposphere/lower stratosphere (CARIBIC)

- All the considered oxidation mechanisms (O_3, OH, Br) succeed to different degree reproducing temporal variation of measured TGM concentration, in particular, the concentration gradient between the troposphere and the stratosphere.
- The highest correlation was obtained for the runs governed by the O_3 chemistry; only slightly lower correlation characterises the simulations with Hg oxidation by atomic Br, whereas the OH chemistry commonly produces poor correlation between the model and observations.